ISSN 0006-2979, Biochemistry (Moscow), 2019, Vol. 84, No. 6, pp. 617-626. © Pleiades Publishing, Ltd., 2019.
Published in Russian in Biokhimiya, 2019, Vol. 84, No. 6, pp. 795-807.
Originally published in Biochemistry (Moscow) On-Line Papers in Press, as Manuscript BM18-334, April 29, 2019.

Defective Central Immune Tolerance Induced by High-Dose D-Galactose Resembles Aging

H. M. Du[1,2,a], Y. J. Wang[1,b], X. Liu[1,c], S. L. Wang[2,d], S. M. Wu[3,e], Z. Yuan[3,f], and X. K. Zhu[1,g]*

[1]*Research Center, Shengjing Hospital of China Medical University, Economic Development Zone, 117000 Benxi, China*
[2]*Department of Oncology, Shengjing Hospital of China Medical University, 110022 Shenyang, China*
[3]*Department of Blood Transfusion, Shengjing Hospital of China Medical University, 110022 Shenyang, China*
[a]*e-mail: dhmcmu@163.com*
[b]*e-mail: 742032002@qq.com*
[c]*e-mail: Sherryliu779122290@qq.com*
[d]*e-mail: doctorwangsl@hotmail.com*
[e]*e-mail: smwu@cmu.edu.cn*
[f]*e-mail: yuan._zhe@163.com*
[g]*e-mail: zhuxk@sj-hospital.org*

Received December 4, 2018
Revised February 12, 2019
Accepted February 12, 2019

Abstract—D-Galactose (D-Gal) promotes accumulation of reactive oxygen species and formation of advanced glycation end-products, ultimately resulting in oxidative stress. D-Gal has been widely used to induce accelerated aging in anti-aging medical research. Although thymic epithelial cells are particularly sensitive to oxidative stress, there are few reports on the thymus changes accompanying D-Gal-induced aging in mice. To study the effect of D-Gal on rodent thymus, we investigated the degree of thymus atrophy and changes in the atrophy relative index in C57BL/6J mice following subcutaneous injection of D-Gal at different doses (200, 500, 1000 mg/kg per day) for 60 days. Compared with the vehicle-treated (0.9% saline) and young controls, D-Gal at doses of 500 and 1000 mg/kg per day led to a significant thymic atrophy; the latter dose caused atrophy similar to that observed in naturally aged (18-20-month-old) mice. Mice treated with high-dose D-Gal exhibited greater immunosenescence, defective central immune tolerance, increased levels of activated splenic immune cell, and chronic low-grade inflammation, i.e., outcomes similar to those observed in natural aging in mice. Taken together, our results indicate that mice treated with high-dose D-Gal may be a valid model for studying induced thymic atrophy and effects of aging on the immune system.

DOI: 10.1134/S000629791906004X

Keywords: D-galactose, oxidative stress, thymic aging, central immune tolerance, negative selection

The world's population is aging; the percentage of individuals >60 years has increased from 9.2% in 1990 to 11.7% in 2013 and is projected to reach 21.1% (>2 billion) by 2050 [1]. As aging is accompanied by many diseases such as cardiovascular and cerebrovascular disorders, type 2 diabetes, cancer, etc., researchers have been investigating factors that promote health in later life and/or protect against age-related diseases.

Numerous studies have shown that reactive oxygen species (ROS) play an important role in aging [2-4]. Oxidative stress, which is recognized as a disruption of redox signaling and control mechanisms leading to aging-associated diseases, not only induces progressive accumulation of macromolecular damage, but also causes progressive pro-oxidizing shift in the redox state of cells, resulting in a decline in the functional efficiency of various cellular processes [3]. The redox theory of aging developed based on the broadening understanding of oxidative stress mechanisms [5-7] suggests that age-associated changes in the redox network structures accompany many pathologies, including type 2 diabetes, non-alcoholic fatty liver disease, atrial fibrillation, and other pro-inflammatory/fibrotic disorders [3]. To better

Abbreviations: D-Gal, D-galactose; MDA, malondialdehyde; NS, normal saline; ROS, reactive oxygen species; RTE, recent thymic emigrant; SAMP, senescence-accelerated mouse prone (model); SOD, superoxide dismutase; TEC, thymic epithelial cell; TRA, tissue-restricted antigen; tT_{reg}, thymic regulatory T cell.

* To whom correspondence should be addressed.

explore this theory in the context of potential aging-associated changes in the host resistance, a mouse model of D-Gal-induced aging was developed [8].

Compared with the natural and senescence-accelerated mouse prone (SAMP) aging models [9, 10], the D-Gal-induced model is convenient, inexpensive, stable, and already widely used. At the normal D-Gal intake typical for humans (50 g/day for healthy adult) [11], D-Gal can be metabolized; an excess of this sugar is converted into galactitol that is accumulated in cells and can induce osmotic stress/ROS formation [8]. Chronic D-Gal exposure in the D-Gal-induced mouse model results in neurological impairments, decreased activity of the anti-oxidant enzymes, and poor immune response, i.e., outcomes that resemble those associated with a normal aging process. Accordingly, this model has been used widely in brain aging and in anti-aging pharmacology studies [8], as well in the studies of heart [12], liver [13], kidney [14], and skin [15] aging. To date, there are very few reports on changes in the immune system in the D-Gal-induced aged hosts, especially mice [16, 17].

Aging affects all body tissues and organs, but thymus represents a unique paradigm, as its age-related degeneration is evident following puberty [18]. However, it is also important to emphasize that thymus continues to involute with aging, when the levels of sex hormones dramatically decline [19]. Indeed, thymic epithelial cells (TECs) may be especially sensitive to damage induced by inflammation and damage-associated molecules, such as ROS [20]. It was demonstrated recently that TECs are deficient with respect to the H_2O_2-reducing enzyme catalase, offering another mechanistic explanation for the accelerated involution of the thymus [20]. Consistent with the idea TECs are highly sensitive to the damage induced by aerobic metabolism is the observation that TEC degeneration is accelerated in obese and leptin-resistant individuals [21]. Moreover, Uddin et al. showed that D-Gal-treated mice develop histological changes in the thymic cortical and medullary regions that resemble aging [16].

As the thymic epithelium has a key role in elimination of autoreactive clones of T cells, thymic atrophy induced by the post-natal TEC homeostatic defects or natural aging impairs the establishment of central immune tolerance. This occurs in part by thymocyte negative selection and generation of thymic regulatory $CD4^+$ T cells (tT_{reg}) [22]. A defect in the central immune tolerance, in turn, can amplify chronic inflammation via increased release from the thymus of autoreactive T cells capable of infiltrating non-lymphoid tissues and inducing inflammatory response. Such events are accompanied by an increase in the production of tumor necrosis factor (TNF)-α and interleukin (IL)-6. This type of induced chronic inflammation in the elderly is now termed *inflamm-aging* [23, 24].

Thus, during aging, thymic atrophy may give rise to the chronic inflammation secondary to the impairment of the overall immune tolerance. Although D-Gal can induce thymic atrophy and affect central immune tolerance in a manner that appears to be similar to that typical for natural aging, this possibility has not been validated experimentally. In the present study, we investigated the relationship between thymus atrophy and D-Gal-induced oxidative stress. In addition, the influence of D-Gal on the central immune tolerance was assessed to ascertain whether D-Gal-treated mice could be a valid model for studying thymic atrophy and effects of aging.

MATERIALS AND METHODS

Animals and treatments. C57BL/6 female mice [25] (19-21 g, 6-week-old) were purchased from Huafukang Bioscience (China) and maintained at the Experimental Research Center of Shengjing Hospital under specific pathogen-free conditions. The mice were provided *ad libitum* access to standard rodent chow and filtered water and maintained in a 12-h-light/dark room at 22°C with a 50% relative humidity. After 2 weeks of adaptation, the now 2-month-old mice were given one of the following preparations daily for 60 days by subcutaneous injection: 0.1 ml normal saline (NS; vehicle control; $n = 16$) or 0.1 ml of D-Gal solution in NS in a dose of 200, 500, or 1000 mg/kg ($n = 16$ in each dose group) (D-Gal solution was made fresh each week). In parallel, 2-month-old mice ($n = 16$) were housed untreated for 60 days and included as "young" comparative controls. Aged female C57BL/6 mice (16-18-month-old; $n = 16$) were purchased from the Nanjing Medical University and housed untreated for the entire study period for eventual inclusion in the analysis (very-aged comparative controls). On the day after the final treatment, all control, D-Gal-treated (now 4-month-old), "young" comparative controls (now 4-month-old), and very-aged mice (now 18-20-month-old) were euthanized by intraperitoneal injection of a pentobarbital overdose; the chest cavity was opened, and the blood was collected from the heart. Serum was isolated from each sample by centrifugation (3000 rpm, 15 min, 4°C) in a Micro 2R system (Thermo Scientific, Germany) and stored at −80°C for subsequent analyses. Immediately thereafter, the thymus and the spleen from each mouse were collected, weighed, and processed as outlined below.

Reagents and antibodies. D-Gal from Sigma (Germany); malondialdehyde (MDA) and superoxide dismutase (SOD) assay kit from Nanjing Jiancheng Bioengineering Institute (Nanjing, China); mouse IL-6 ELISA kit from BD Biosciences (USA); Red Blood Cell (RBC) lysis buffer, Bicinchoninic Acid (BCA) protein assay kit, and SDS-PAGE materials from Beyotime (China); Mouse 1X Lymphocyte Separation Medium from Dakewe Biosciences (China); Cell Activation Cocktail (with 2.5 mg/ml brefeldin A) and True Nuclear

Transcription Factor Buffer from Biolegend (USA) were used in this study. For flow cytometry analyses, fluorochrome-conjugated rabbit antibodies against mouse cell surface markers were purchased from Biolegend. These included phycoerythrin (PE)- or fluorescein isothiocyanate (FITC)-conjugated anti-CD4 (clone GK1.5; conjugate used depended on specific experiment), FITC-anti-CD8 (clone 53-6.7), PE-anti-CD28 (clone 37.51), Alexa Fluor (AF)-647-anti-CD44 (clone IM7), PE-anti-Ki67 (clone 16A8), allophycocyanin (APC)-anti-TNFα (clone MP6-XT22), PE-anti-CD25 (clone PC61), PE-anti-CD3 (clone 17A2), and AF-647-anti-Foxp3 (clone 150D). Primary rabbit anti-mouse antibodies from Proteintech (USA) for the use in Western blot analyses were anti-autoimmune regulator (AIRE) (polyclonal, 22517-1-AP) and anti-GAPDH (monoclonal, 60004-1-Ig). Horseradish peroxidase (HRP)-conjugated goat anti-rabbit IgG was purchased for the use as the secondary antibody.

Flow cytometry assay. At necropsy, one half of each thymus (lobe) and one half of each spleen from each mouse were isolated to be used in flow cytometry analysis; the remainder was used for the assays below. Single-cell suspensions were prepared from each thymic and splenic sample using a 70-μm cell strainer. EDTA-anticoagulated blood and spleen cells were erythrocyte-depleted using RBC lysis buffer, and the final cell pellet was then washed with the staining buffer. After determining cell concentrations using a hemocytometer, aliquots of each sample (10^6 cells) were stained with individual specific antibodies against given cell surface CD markers (on ice, in the dark, 20 min, using the amount of antibody recommended by the manufacturer). Parallel aliquots (10^6 cells) were fixed and permeabilized with 75% ethanol for 1 h and then stained intracellularly for Ki-67 (on ice, in the dark, 30 min, with the recommended antibody amount). The final set of cells was fixed and permeabilized with True-Nuclear Transcription Factor Buffer before intracellular staining for Foxp3 (all steps were the same as in the analysis of Ki-67 expression).

To stain cells for TNFα, one half of each spleen was ground in 5 ml of Mouse Lymphocyte Separation Medium (ρ = 1.081 g/ml) and passed through a 70-μm cell strainer. The suspension was transferred immediately to a 15 ml centrifugal tube and gently overlaid with serum-free RPMI 1640, centrifuged at 800*g* (30 min, 4°C), and the resulting supernatant containing lymphocytes was collected. After the final centrifugation/washing with phosphate-buffered saline (PBS), the lymphocytes were suspended in Cell Activation Cocktail containing 2.5 mg/ml brefeldin A and counted with a hemocytometer, and then aliquots of cells (10^6 cells) were incubated for 6 h in an incubator in 5% CO_2 at 37°C. The samples were then collected, centrifuged/washed with PBS, and stained with anti-CD3 or anti-CD8 antibodies (on ice, in the dark, 20 min, using recommended antibody amount). The cells were then pelleted, fixed in 2% paraformaldehyde, permeabilized with 0.1% Triton X-100, and treated with anti-TNFα (on ice, in the dark, 30 min, using recommended antibody amount).

After staining, the cells were analyzed by flow cytometry using a FACSCalibur (BD Biosciences, USA). All generated data was processed with the system-associated FlowJo software. A minimum of 10,000 events/sample were acquired.

Biochemical analysis of SOD and MDA in the serum. SOD activity and MDA content in the serum were evaluated colorimetrically using commercial kits. All absorbance measurements were done using a Synergy H1 plate reader (BioTek, USA). The level of IL-6 in the serum was measured using an ELISA kit (BD Biosciences) following manufacturer's instructions (the detection limit of the used kit was 3.8 pg/ml).

Western blot analysis. Total protein in the remaining unused portion of each isolated thymus was extracted using radioimmunoprecipitation assay (RIPA) lysis buffer (1 ml of buffer per 100 mg tissue; Beyotime, China) according to manufacturer's protocols. Total protein concentration in each extract was then quantified using a BCA assay kit, and aliquots containing 30 μg protein were loaded into/resolved in SDS-PAGE gels. After resolution, the proteins were electrotransferred to a polyvinylidene fluoride (PVDF) membrane (Millipore, USA) that was then blocked at room temperature for 2 h in a solution of 5% fat-free dried milk in Tris-buffered saline containing 0.1% (v/v) Tween 20 (TBST, pH 7.5). Each membrane was then incubated overnight at 4°C with specified antibodies (at 1 : 2000 dilution). After gentle rinsing with TBST to remove unbound primary antibody, each membrane was incubated for 2 h at room temperature in TBST containing HRP-conjugated anti-rabbit IgG (1 : 40,000). In all cases, the membranes were also probed for GAPDH as the loading control. After a final rinse with TBST, each membrane was treated with enhanced chemiluminescence reagent (Thermo Scientific) and evaluated in a C300 chemiluminescence imaging system (Azure, USA) using Image J software (National Institutes of Mental Health, Washington, D.C., USA).

Statistical analysis. The data for each study parameter from each group are presented as mean ± SD. Analysis of differences among the treated groups and controls was conducted using the one-way analysis of variance (ANOVA). The differences were considered significant at p-values < 0.05. Data analysis was performed using Prism v. 5.0 (GraphPad, USA).

RESULTS

Oxidative stress and thymic atrophy induced by D-Gal in mice resemble the age-associated ones. The activity of SOD and the MDA content in the serum were measured

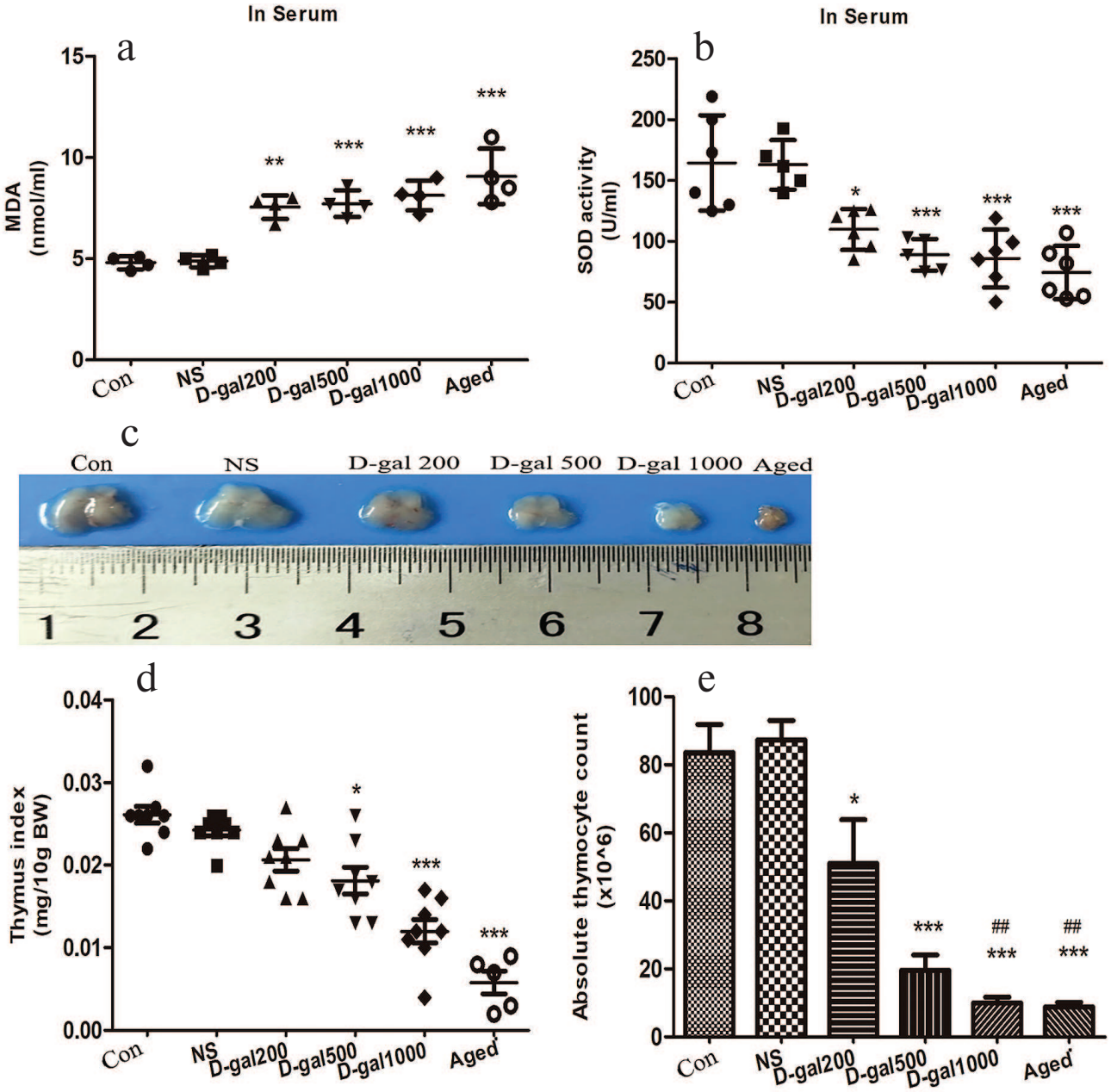

Fig. 1. Oxidative stress and thymic atrophy induced by D-Gal (daily, 60 days) in C57/BL6 mice. a) MDA content in the serum of 4-month-old mice treated with D-Gal (200, 500, and 1000 mg/kg daily), "young" controls (Con, 4-month-old), vehicle-only controls (NS), and aged controls (Aged, 18-20-month-old). b) SOD activity in the serum. c) Representative images of the thymus. d) Thymic indices. e) Absolute thymocyte numbers. * $p < 0.05$; ** $p < 0.01$; *** $p < 0.001$ vs. Con and NS; $^{\#\#}$ $p < 0.01$ vs. 200 mg D-Gal/kg daily.

to assess if D-Gal induced aging in the used mouse model. Conservative D-Gal doses of 50 and 200 mg/kg per day were first evaluated in a pilot assay. Although increased MDA formation and downregulation of SOD activity were observed for both doses (data not shown), there was no visible thymic atrophy. Therefore, the doses of 200, 500, and 1000 mg/kg daily were used to determine whether the effect of D-Gal was dose-dependent and whether higher doses of D-Gal induced thymic atrophy. As seen in Fig. 1, a and b, treatment with D-Gal significantly increased MDA levels and reduced SOD activity in the blood of now 4-month-old mice compared to the "young" and vehicle-only-treated controls (also now 4-month-old). At the two highest D-Gal doses tested (500 and 1000 mg/kg daily), the decreased levels of SOD activity were similar to those observed in naturally very-aged (18-20-month-old) controls; the MDA levels seen across the three tested doses were on par with those in the aged controls. Each of the two highest doses induced thymic atrophy (Fig. 1c), with the 1000 mg/kg daily dose having

the greatest impact. Accordingly, both thymic index (thymus weight/10 g body weight) (Fig. 1d) and absolute thymocyte counts (Fig. 1e) were maximally decreased in this highest-dose group.

Immunosenescence induced by D-Gal resembles that associated with natural aging. A hallmark of immunosenescence is accumulation of highly differentiated effector $CD8^+$ T cells lacking CD28, a vital co-stimulatory molecule needed for T cell receptor (TCR)-mediated activation. Accumulation of $CD8^+CD28^-$ T cells ("senescent" cells) is associated with high inflammation levels and increased risk of age-related diseases and mortality. Here, naturally very-aged (18-20-month-old) mice showed clear increase in the levels of senescent cells in their blood relative to the 4-month-old controls (Fig. 2, a and b). The levels of senescent cells were also upregulated in the blood of mice treated with D-Gal (500 and 1000 mg/kg daily) as compared to the vehicle-only and "young" controls, indicating that high doses of D-Gal induced the processes similar to those occurring during natural aging.

Increase in the content of activated immune cells and chronic low-grade inflammation in D-Gal-treated and naturally aging mice. Reduced levels of recent thymic emigrants (RTEs), a high proportion of $CD44^{hi}$ cells (reflect antigen-experienced T cells), RTEs with increased proliferative activity ($Ki67^+$), and $CD4^+/CD8^+$ RTEs (from the atrophied thymus) with activated immune cell phenotypes (potential autoreactive cells) can indicate *in situ* alterations that lead to the reduced immune function. We observed increased levels of activated ($CD4^+CD44^{hi}Ki67^+$ and $CD8^+CD44^{hi}Ki67^+$) cells, especially in the mice that received the highest D-Gal dose (Fig. 3, a-d). These levels were on par with those measured in naturally aged mice.

To ascertain if there were any changes in systemic inflammation in the mice treated with D-Gal or naturally aged animals, the serum levels of the key inflammatory cytokine IL-6 and the contents of TNFα-producing $CD4^+$ splenocytes were also evaluated. The IL-6 levels in the serum were notedly elevated in a non-dose-related manner in all D-Gal-treated groups and naturally aged mice (Fig. 3e). At the same time, the percentage of splenic $CD4^+TNF\alpha^+$ T cells was significantly increased in mice treated with D-Gal (500 and 1000 mg/kg daily) and in naturally aged mice (relative to the vehicle-only and young control mice) (Fig. 3, f and g). The values observed for these two higher doses were on par with the values in the older controls.

D-Gal-treated mice show impaired clonal deletion of single-positive (SP) thymocytes due to defects in the negative selection that resemble those associated with aging. The ability of D-Gal-induced atrophied thymus to host negative selection processes was evaluated. A significant reduction in the percentage of $CD4^+CD8^+$ double-positive (DP) thymocytes was noted in thymuses from the mice treated with 1000 mg D-Gal/kg daily compared to the thymuses obtained from vehicle-only/young controls and mice that received the two lower D-Gal doses (Fig. 4, a and b). Accordingly, it was expected that there would be an equal reduction in the levels of CD4 and CD8 single-

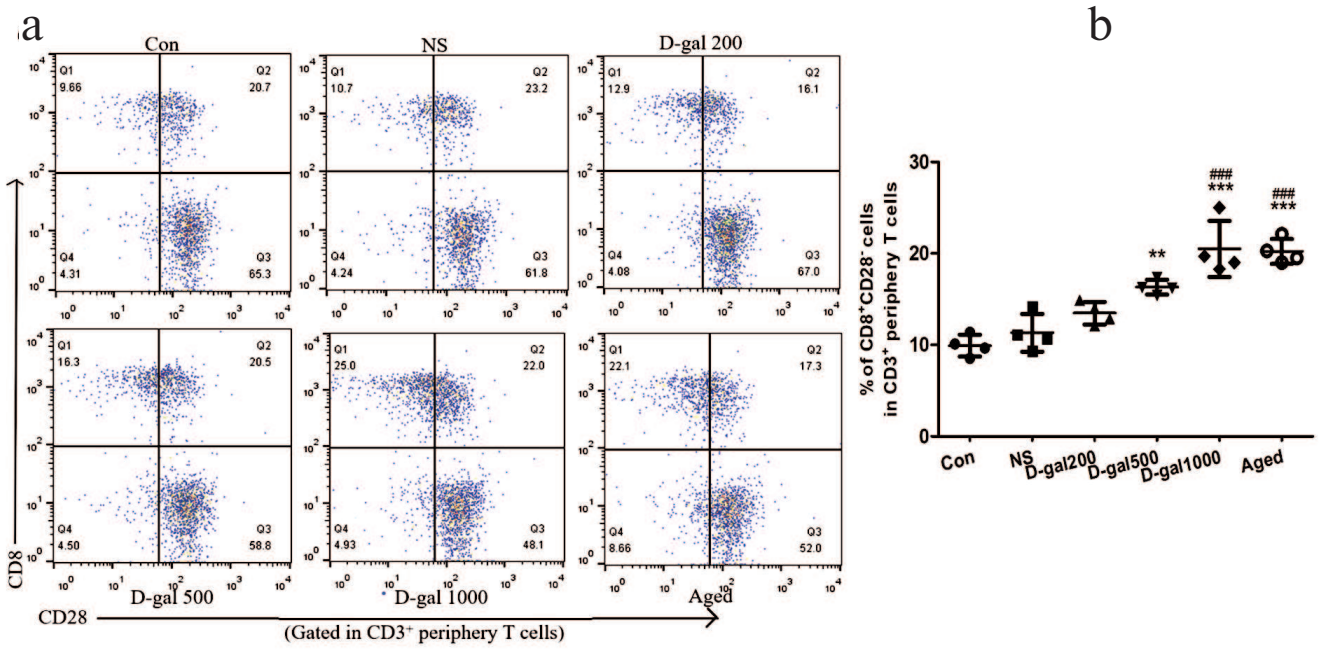

Fig. 2. Immunosenescence induced by D-Gal (daily, 60 days) in C57/BL6 mice. a) Representative dot-plots of $CD3^+CD8^+CD28^-$ cells (left upper quadrant) gated in peripheral $CD3^+$ T cells (in blood) from D-Gal-treated/control mice. b) Percentages of $CD8^+CD28^-$ cells among peripheral $CD3^+$ T cells. ** $p < 0.01$; *** $p < 0.001$ vs. Con and NS; ### $p < 0.001$ vs. 200 mg D-Gal/kg daily.

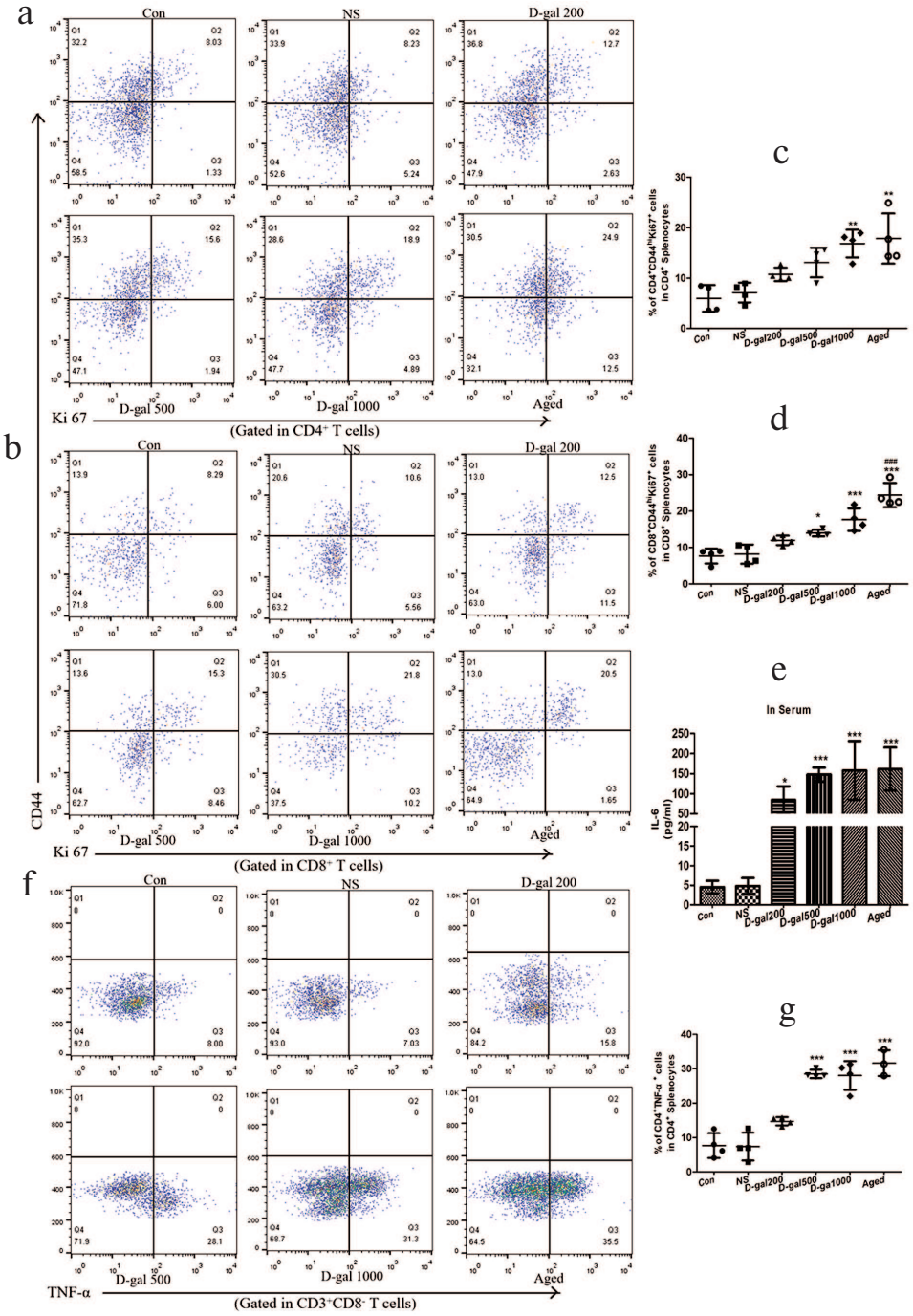

Fig. 3. Activated immune cells and chronic low-grade inflammation induced by D-Gal (60 days) in C57/BL6 mice. a) Representative dot-plots of $CD44^{hi}Ki67^{+}$ cells (right upper quadrant) gated in $CD4^{+}$ peripheral T-cells (in splenocytes) from D-Gal-treated and control mice. b) Representative dot-plots of $CD44^{hi}Ki67^{+}$ cells (right upper quadrant) gated in $CD8^{+}$ peripheral T-cells (in splenocytes) from D-Gal-treated and control mice. c, d) Percentage of $CD44^{hi}Ki67^{+}$ cells in peripheral $CD4^{+}$ and $CD8^{+}$ T cells. e) Serum IL-6 (pg/ml). f) Representative dot-plots of $TNF\alpha^{+}$ cells among peripheral $CD4^{+}$ T cells (in splenocytes). Note: during the process of TNFα activation, Cell Activation Cocktail can downregulate CD4 expression; therefore, we used the $CD3^{+}CD8^{-}$ T cell subset to represent the $CD4^{+}$ subset. g) Percentage of $CD4^{+}TNF\alpha^{+}$ cells in $CD4^{+}$ T cells. * $p < 0.05$; ** $p < 0.01$; *** $p < 0.001$ vs. Con and NS; $^{###}p < 0.001$ vs. 200 mg D-Gal/kg daily.

positive (SP) subpopulations in these highest-dose/naturally very-aged groups. Interestingly, the prevalence of both CD4 and CD8 SP thymocytes was increased in the atrophied thymuses of the mice treated with the highest D-Gal dose, as well as in the thymuses of naturally very-aged mice (Fig. 4, a, c, and d). Such outcomes indicated that the atrophied thymuses did not efficiently perform clonal deletion (negative selection).

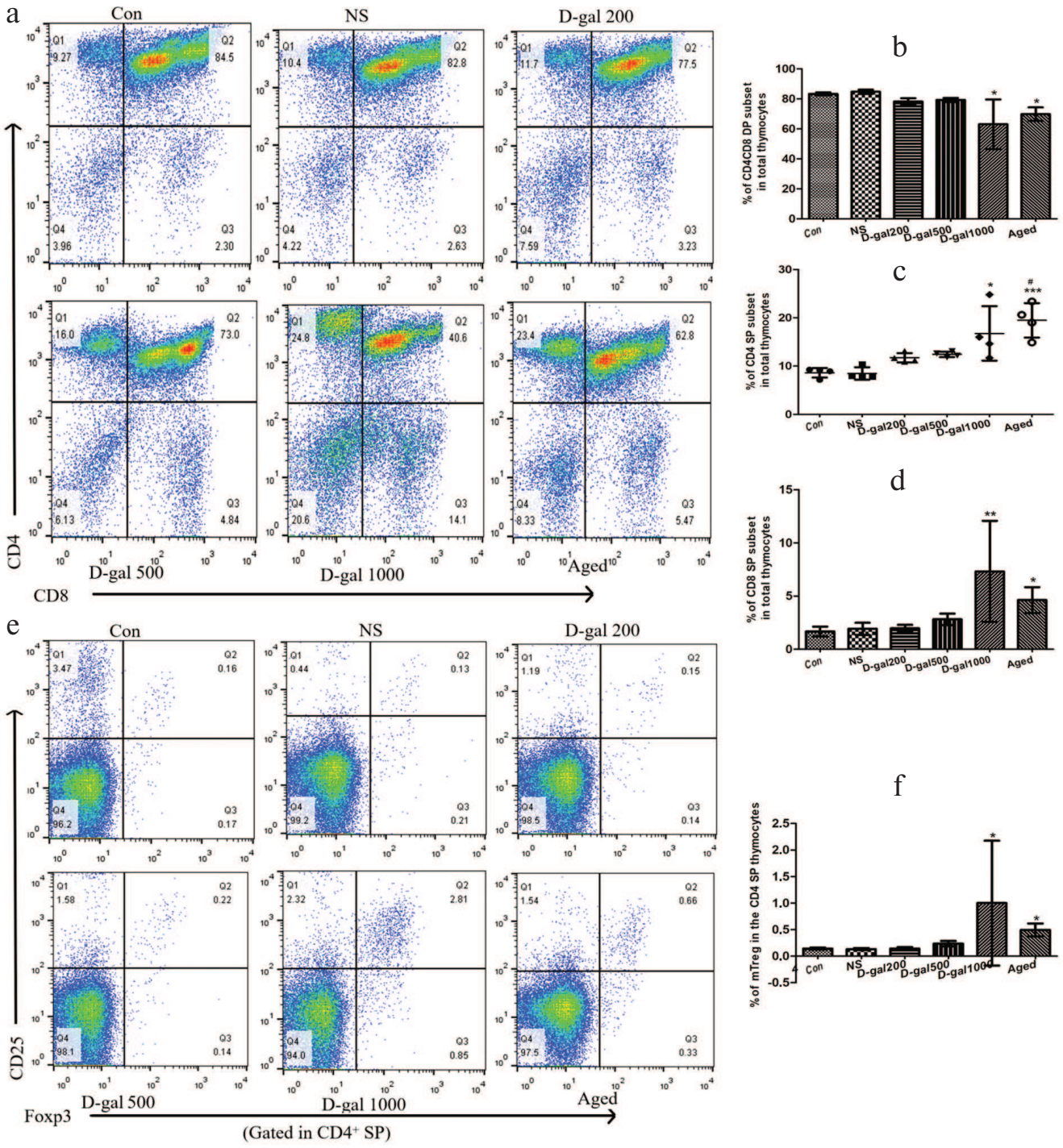

Fig. 4. Effects of different D-Gal doses (daily, 60 days) on the central immune tolerance in mice. a) Representative dot-plots of the CD4CD8 DP cell subset ($CD4^+CD8^+$, right upper quadrant), CD4 SP cell subset ($CD4^+CD8^-$, left upper quadrant), and CD8 SP cell subset ($CD4^-CD8^+$, right lower quadrant) among the mouse thymocytes. b-d) Percentage of DP, CD4 SP, and CD8 SP cells in thymocytes. e) Representative dot-plots of $CD25^+Foxp3^+$ cells (right upper quadrant) in CD4 SP thymocytes. f) Percentage of $CD4^+CD25^+Foxp3^+$ cells in CD4 SP thymocytes. * $p < 0.05$; ** $p < 0.01$; *** $p < 0.001$ vs. Con and NS; $^{\#}p < 0.05$ vs. 200 and 500 mg D-Gal/kg daily.

Impairments in the negative selection were not accompanied by a deficiency in the tT_{reg} cells in the thymus. In fact, the content of these cells increased in naturally-aged mice and mice treated with 1000 mg D-Gal/kg compared with tissues obtained from the vehicle only/"young" controls and mice that received the two lower D-Gal doses (Fig. 4, e and f). It appears that in these D-Gal-treated mice, as well as in naturally very-

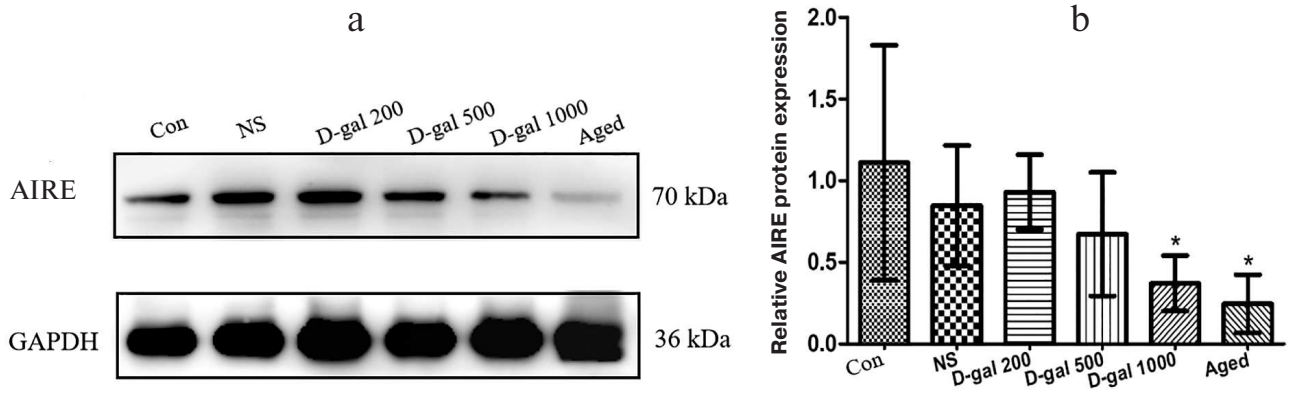

Fig. 5. Effects of D-Gal treatment on AIRE expression in the thymus. a) Representative Western blot of thymic extract stained for AIRE and GAPDH. b) Relative AIRE levels in mice. * $p < 0.05$ vs. Con, NS, and 200 D-Gal/kg per day.

aged controls, impaired central immune tolerance and disrupted negative selection were balanced by an enhanced tT_{reg} cell generation.

AIRE downregulation in mTECs of D-Gal-treated mice resembles the one seen in aging. Induction of immune tolerance in the thymus requires presentation of tissue-restricted antigens (TRAs) to developing thymocytes, which promotes clonal deletion of T cells reactive to self-antigens. AIRE is a transcription factor expressed by mTECs to promote ectopic TRA expression; mTEC subsets that express AIRE are crucial for negative selection. In the current study, we observed an impairment of negative selection in the thymus of mice that had received the highest D-Gal dose (see above), and it appears that this impairment might be partially attributed to AIRE deficiency (Fig. 5, a and b). Specifically, relative expression levels of AIRE in the thymic cells in these mice were on par with the levels observed in naturally aged mice (albeit the Western blot itself seems to show far lesser expression in the samples from these controls). In either case, these values were all significantly lower compared to those in the vehicle only/young controls and mice that received the two lower D-Gal doses.

DISCUSSION

In this study, we compared the degree of thymic atrophy in the mouse model of accelerated aging induced by D-Gal. The doses of 500 and 1000 mg/kg daily for 60 days induced significant thymus atrophy (especially, the higher dose) to a degree similar to that seen in naturally aged mice (18-20-month-old). Consistent with this change, there was also a decline in the thymic index and thymocyte count in these mice, together with greater immunosenescence. In accordance with the thymus atrophy, the affected mice also displayed impaired negative selection, an increase in the number of activated immune cells, and chronic low-grade inflammation, i.e., outcomes that parallel events seen as a result of natural aging.

D-Gal is a reducing sugar metabolized by D-galactokinase or galactose-1-phosphate uridyl transferase at physiologically normal concentrations in the body. Any excess of D-Gal is converted to galactitol, the accumulation of which in cells can induce osmotic stress and ROS production [8]. D-Gal also reacts with free amino groups of amino acids with the formation of advanced glycation end-products (AGE) that can stimulate free radical production (events implicated in aging and age-related diseases) [26]. Both ROS accumulation and AGE formation ultimately result in the oxidative stress. Two aspects of oxidative stress are currently recognized: one is the damage of macromolecules (original concept) and the other is disruption of redox signaling and regulatory mechanisms leading to age-related diseases [3]. The redox theory of aging recognizes that organisms have evolved in the O_2-rich environments, which has created a critical redox interface between an organism and its surroundings. Redox elements are present throughout metabolic/structural systems that operate as functional networks to support genome in the adaptation to the environment and various challenges [3]. Compared with continuous lifelong exposure to oxidative challenges during natural growth/aging, repetitive D-Gal exposure over a relatively short time (e.g., 60 days) can accelerate the process of aging. Many studies have shown that D-Gal-treated animals resemble aged control counterparts (16- to 24-month-old) [16, 27]. This accelerated aging model has been demonstrated to be reliable for mimicking natural aging.

One of the obvious features of aging is progressive age-related thymus atrophy (involution). Thymus atrophy may be attributed to several key contributors, including hormones, glucocorticoids, chemo-/radiotherapy, and/or oxidative stress [28]. Unlike naturally occurring processes, glucocorticoid and pharmacologic therapies act on developing T cells [22, 29] and so any impact on

TECs is mainly secondary due to the loss of crosstalk (e.g., CD40 and/or RANK stimuli). In comparison, oxidative stress may influence TECs directly [20] and cause acute or chronic atrophy, which might explain why there is continuous thymus atrophy with aging, even when the levels of sex hormones markedly decline [19].

The organization of a mature thymus reflects requirements for specialized intra-thymic microenvironment that supports step-wise development of T cells [22]. In the cortex, a 3D network of cortical thymic epithelial cells (cTECs) enables multiple interactions with $CD4^{-}CD8^{-}$ (double-negative, DN) and $CD4^{+}CD8^{+}$ (double-positive, DP) immature thymocytes. In the medulla, subsets of mTECs interact with more mature thymocyte subsets, including CD4/CD8 SP and $CD4^{+}Foxp3^{+}$ regulatory (T_{reg}) cells. Cortical DP thymocytes that experience αβT-cell receptor (TCR) signals in response to self-peptides presented by the major histocompatibility complex (MHC) proteins can undergo positive selection, resulting in maturation and commitment to either CD4 or CD8 lineages [30]. Newly selected SP thymocytes are not yet fully mature, and so do not respond to TCR triggering by proliferation [31]. This delay in the acquisition of functional competence allows the high-affinity αβTCR signaling to trigger apoptosis (i.e., negative selection), to eliminate self-reactive thymocytes from the repertoire [32], and so to enforce self-tolerance.

AIRE is a transcription factor expressed by mTECs that promotes ectopic expression of TRAs [33, 34]. A particular mTEC subset that expresses AIRE and can present TRAs is crucial for the negative selection. AIRE-deficient mice exhibit a reduction in the TRA expression and display the autoimmune phenotype with autoantibody production and inflammatory cell infiltration into various tissues, including the pancreas and lacrimal glands [35, 36]. Conceptually, AIRE may prevent autoimmunity by promoting both recessive and dominant mechanisms of tolerance, by driving deletion of thymocytes reactive to promiscuously expressed TRAs, or by inducing differentiation of such thymocytes into the tT_{reg} cell lineage [34].

It was expected here that thymus atrophy in naturally aged mice or mice with accelerated aging might be accompanied by impairments in the central immune tolerance. Indeed, impairments in the central immune tolerance due to the defective negative selection were seen in both models, and it appears that such impairments might be partially attributed to AIRE deficiency. The current study also showed that thymic atrophy positively influenced tT_{reg} cell generation. As seen by Oh et al. [37], increased peripheral T_{reg} cells in aged mice do not re-enter the aged thymus to augment inhibition of new tT_{reg} cell generation. Based on that, we concluded that the atrophied thymus may attempt to balance defective negative selection by enhancing tT_{reg} cell generation to maintain central T cell tolerance and, further, that once the balance is upset, age-related diseases could potentially occur.

In summary, this study demonstrated that thymic atrophy could be induced in mice by repeated (daily, 60 days) administration of a high dose of D-Gal, and that this atrophy was mainly caused by the oxidative stress. Such outcomes not only mimicked but seemed to accelerate the natural aging process in hosts. High-dose D-Gal treatment also resulted in defective central immune tolerance, which was manifested as impaired negative selection, increased levels of activated immune cells in the spleen, and induction of inflammation, i.e., outcomes similar to those occurring during natural aging. It is difficult to determine whether senescence caused the thymic atrophy or vice versa. Still, it is clear from these studies that delay in the thymic atrophy or increase in the content of anti-oxidants in a host might be effective countermeasures to inflamm-aging and potentially postpone induction of expected immunosenescence.

Funding. This work was supported by the National Natural Science Foundation of China (grant no. 81270430).

Acknowledgements. The authors wish to thank the International Science Editing (http://www.international-scienceediting.com) for their assistance in the preparation of this manuscript.

Conflict of interest. The authors declare no conflict of interest.

Ethical approval. All mice were handled humanely following the protocols approved by the Experiment Animal Center of China Medical University in accordance with the recommendations in the Guide for the Care and Use of Laboratory Animals of the National Institutes of Health.

REFERENCES

1. Sander, M., Oxlund, B., Jespersen, A., Krasnik, A., Mortensen, E., Westendorp, R., and Rasmussen, L. (2015) The challenges of human population ageing, *Age Ageing*, **44**, 185-187; doi: 10.1093/ageing/afu189.
2. De Martinez, T. I., and de la Fuente, M. (2015) The role of Hsp70 in oxi-inflamm-aging and its use as a potential biomarker of lifespan, *Biogerontology*, **16**, 709-721; doi: 10.1007/ s10522-015-9607-7.
3. Go, Y., and Jones, D. (2017) Redox theory of aging: implications for health and disease, *Clin. Sci.*, **131**, 1669-1688; doi: 10.1042/CS20160897.
4. Guzik, T., and Cosentino, F. (2018) Epigenetics and immunometabolism in diabetes and aging, *Antioxid. Redox Signal.*, **29**, 257-274; doi: 10.1089/ars.2017.7299.
5. Jones, D., and Sies, H. (2015) The redox code, *Antioxid. Redox Signal.*, **23**, 734-746; doi: 10.1089/ars.2015.6247.
6. Jones, D. (2016) Hydrogen peroxide and central redox theory for aerobic life: a tribute to Helmut Sies: scout, trailblazer, and redox pioneer, *Arch. Biochem. Biophys.*, **595**, 13-18; doi: 10.1016/j.abb.2015.10.022.

7. Sies, H. (2017) Hydrogen peroxide as a central redox signaling molecule in physiological oxidative stress: oxidative eustress, *Redox Biol.*, **11**, 613-619; doi: 10.1016/j.redox. 2016.12.035.
8. Shwe, T., Pratchayasakul, W., Chattipakorn, N., and Chattipakorn, S. (2018) Role of D-galactose-induced brain aging and its potential used for therapeutic interventions, *Exp. Gerontol.*, **101**, 13-36; doi: 10.1016/j.exger.2017.10.029.
9. Li, M., Guo, K., Adachi, Y., and Ikehara, S. (2016) Immune dysfunction associated with abnormal bone marrow-derived mesenchymal stroma cells in senescence accelerated mice, *Int. J. Mol. Sci.*, **17**, E183; doi: 10.3390/ijms17020183.
10. Currais, A., Farrokhi, C., Dargusch, R., Armando, A., Quehenberger, O., Schubert, D., and Maher, P. (2018) Fisetin reduces the impact of aging on behavior and physiology in the rapidly aging SAMP8 mouse, *J. Gerontol. A Biol. Sci. Med. Sci.*, **73**, 299-307; doi: 10.1093/gerona/ glx104.
11. Morava, E. (2014) Galactose supplementation in phosphoglucomutase-1 deficiency: review and outlook for a novel treatable CDG, *Mol. Genet. Metab.*, **112**, 275-279; doi: 10.1016/j.ymgme.2014.06.002.
12. Bo-Htay, C., Palee, S., Apaijai, N., Chattipakorn, S., and Chattipakorn, N. (2018) Effects of D-galactose-induced aging on the heart and its potential interventions, *J. Cell. Mol. Med.*, **22**, 1392-1410; doi: 10.1111/jcmm.13472.
13. Wang, H., Hu, L., Li, L., Wu, X., Fan, Z., Zhang, C., Wang, J., Jia, J., and Wang, S. (2018) Inorganic nitrate alleviates the senescence-related decline in liver function, *Sci. China Life Sci.*, **61**, 24-34; doi: 10.1007/s11427-017-9207-x.
14. Mo, Z., Liu, Y., Li, C., Xu, L., Wen, L., Xian, Y., Lin, Z., Zhan, J., Chen, J., and Xu, F. (2017) Protective effect of SFE-CO2 of *Ligusticum chuanxiong* hort against D-galactose-induced injury in the mouse liver and kidney, *Rejuven. Res.*, **20**, 231-243; doi: 10.1089/rej.2016.1870.
15. Li, W., Li, N., Sui, B., and Yang, D. (2017) Anti-aging effect of fullerenol on skin aging through derived stem cells in a mouse model, *Exp. Ther. Med.*, **14**, 5045-5050; doi: 10.3892/etm.2017.5163.
16. Uddin, M., Nishio, N., Ito, S., Suzuki, H., and Isobe, K. (2010) Toxic effects of D-galactose on thymus and spleen that resemble aging, *J. Immunotoxicol.*, **7**, 165-173; doi: 10.3109/15476910903510806.
17. Li, M., Ouyang, W., Li, J., Si, L., Li, X., Guo, J., and Li, H. (2016) Effects of kinetin on thymus and immune function of aging rats, *Pakistan Vet. J.*, **36**, 356-362.
18. Chaudhry, M., Velardi, E., Dudakov, J., and van den Brink, M. (2016) Thymus: the next (re)generation, *Immunol. Rev.*, **271**, 56-71; doi: 10.1111/imr.12418.
19. Cepeda, S., and Griffith, A. (2018) Thymic stromal cells: roles in atrophy and age-associated dysfunction of the thymus, *Exp. Gerontol.*, **105**, 113-117; doi: 10.1016/j.exger.2017.12.022.
20. Griffith, A., Venables, T., Shi, J., Farr, A., van Remmen, H., Szweda, L., Fallahi, M., Rabinovitch, P., and Petrie, H. (2015) Metabolic damage and premature thymus aging caused by stromal catalase deficiency, *Cell. Rep.*, **12**, 1071-1079; doi: 10.1016/j.celrep.2015.07.008.
21. Dixit, V. (2010). Thymic fatness and approaches to enhance thymopoietic fitness in aging, *Curr. Opin. Immunol.*, **22**, 521-528; doi: 10.1016/j.coi.2010.06.010.
22. Abramson, J., and Anderson, G. (2017) Thymic epithelial cells, *Annu. Rev. Immunol.*, **35**, 85-118; doi: 10.1146/annurev-immunol-051116-052320.
23. Franceschi, C., and Campisi, J. (2014) Chronic inflammation (inflammaging) and its potential contribution to age-associated diseases, *J. Gerontol. A Biol. Sci. Med. Sci.*, **69**, Suppl. 1, S4-S9; doi: 10.1093/gerona/glu057.
24. Coder, B., Wang, H., Ruan, L., and Su, D. (2015) Thymic involution perturbs negative selection leading to autoreactive T-cells that induce chronic inflammation, *J. Immunol.*, **194**, 5825-5837; doi: 10.4049/jimmunol.1500082.
25. Markle, J., and Fish, E. (2014) SeXX matters in immunity, *Trends Immunol.*, **35**, 97-104; doi: 10.1016/j.it.2013.10.006.
26. Rehman, S., Shah, S., Ali, T., Chung, J., and Kim, M. (2017) Anthocyanins reversed D-galactose-induced oxidative stress and neuroinflammation mediated cognitive impairment in adult rats, *Mol. Neurobiol.*, **54**, 255-271; doi: 10.1007/s12035-015-9604-5.
27. Cebe, T., Yanar, K., Atukeren, P., Ozan, T., Kuruc, A., Kunbaz, A., Sitar, M., Mengi, M., Aydin, M., and Esrefoglu, M. (2014) Comprehensive study of myocardial redox homeostasis in naturally- and mimetically-aged rats, *Age (Dordr.)*, **36**, 9728; doi: 10.1007/s11357-014-9728-y.
28. Majumdar, S., and Nandi, D. (2018) Thymic atrophy: experimental studies and therapeutic interventions, *Scand. J. Immunol.*, **87**, 4-14; doi: 10.1111/sji.12618.
29. Purton, J., Monk, J., Liddicoat, D., Kyparissoudis, K., Sakkal, S., Richardson, S., Godfrey, D., and Cole, T. (2004) Expression of the glucocorticoid receptor from the 1A promoter correlates with T-lymphocyte sensitivity to glucocorticoid-induced cell death, *J. Immunol.*, **173**, 3816-3824; doi: 10.4049/jimmunol.173.6.3816.
30. Kurd, N., and Robey, E. (2016) T-Cell selection in the thymus: a spatial and temporal perspective, *Immunol. Rev.*, **271**, 114-126; doi: 10.1111/imr.12398.
31. Xing, Y., Wang, X., Jameson, S., and Hogquist, K. (2016) Late stages of T-cell maturation in the thymus involve NF-κB and tonic type I interferon signaling, *Nat. Immunol.*, **17**, 565-573; doi: 10.1038/ni.3419.
32. Klein, L., Kyewski, B., Allen, P., and Hogquist, K. (2014) Positive and negative selection of the T-cell repertoire: what thymocytes see (and don't see), *Nat. Rev. Immunol.*, **14**, 377-391; doi: 10.1038/nri3667.
33. Malchow, S., Leventhal, D., Lee, V., Nishi, S., Socci, N., and Savage, P. (2016) AIRE enforces immune tolerance by directing autoreactive T cells into the regulatory T cell lineage, *Immunity*, **44**, 1102-1113; doi: 10.1016/j.immuni.2016.02.009.
34. Takaba, H., and Takayanagi, H. (2017) The mechanisms of T cell selection in the thymus, *Trends Immunol.*, **38**, 805-816; doi: 10.1016/j.it.2017.07.010.
35. DeVoss, J., LeClair, N., Hou, Y., Grewal, N., Johannes, K., Lu, W., Yang, T., Meagher, C., Fong, L., Strauss, E., and Anderson, M. (2010) An autoimmune response to odorant binding protein 1a is associated with dry eye in the AIRE-deficient mouse, *J. Immunol.*, **184**, 4236-4246; doi: 10.4049/jimmunol.0902434.
36. Hubert, F., Kinkel, S., Crewther, P., Cannon, P., Webster, K., Link, M., Uibo, R., O'Bryan, M., Meager, A., Forehan, S., Smyth, G., Mittaz, L., Antonarakis, S., Peterson, P., Heath, W., and Scott, H. (2009) AIRE-deficient C57BL/6 mice mimicking the common human 13-base pair deletion mutation present with only a mild autoimmune phenotype, *J. Immunol.*, **182**, 3902-3918; doi: 10.4049/jimmunol.0802124.
37. Oh, J., Wang, W., Thomas, R., and Su, D. (2017) Capacity of tT_{reg} generation is not impaired in the atrophied thymus, *PLoS Biol.*, **15**, e2003352; doi: 10.1371/journal.pbio.2003352.